buildings

Article

Numerical Prediction Method for Vibration Characteristics of Steel-Framed Autoclaved Lightweight Aerated Concrete Floor Structures

Haruki Mizunuma [1,*], Takumi Asakura [1,*], Yasuhiko Ishiwatari [2], Takayuki Shiraishi [2] and Fumiaki Satoh [3]

1 Asakura Laboratory, Department of Mechanical Engineering, Graduate School of Science and Technology, Noda Campus, Tokyo University of Science, Chiba 278-0022, Japan
2 CEL Corporation, 3-7-1 Kyobashi, Chuo-ku, Tokyo 104-0031, Japan
3 Faculty of Creative Engineering, Department of Architecture, Chiba Institute of Technology, Chiba 275-0016, Japan
* Correspondence: 7522566@ed.tus.ac.jp (H.M.); t_asakura@rs.tus.ac.jp (T.A.)

check for updates

Citation: Mizunuma, H.; Asakura, T.; Ishiwatari, Y.; Shiraishi, T.; Satoh, F. Numerical Prediction Method for Vibration Characteristics of Steel-Framed Autoclaved Lightweight Aerated Concrete Floor Structures. *Buildings* **2022**, *12*, 1910. https://doi.org/10.3390/buildings12111910

Academic Editors: Sidi Shan and Cuihua Li

Received: 21 September 2022
Accepted: 1 November 2022
Published: 7 November 2022

Abstract: The prediction of floor vibration is of great importance from the viewpoint of accurate prediction of a room's sound environment. Despite the advantage of low cost, because the density and elasticity of autoclaved lightweight aerated concrete (ALC) panels are much lower than those of reinforced-concrete panels, ALC floor structures suffer from weak sound insulation and require better sound insulation design. However, there have been not yet been any studies of sound insulation improvement of steel-framed ALC floor structures, and it is novel to clarify how the floor-impact-sound characteristics are affected by the panel size and beam structure. In this paper, a finite element analysis was applied to the vibration simulation of an ALC floor structure on a steel-framed structure. The validity of the proposed method was firstly confirmed by comparison with measurement results. Furthermore, by using the validated simulation method, the effect of the arrangement of ALC panels and their supporting steel-framed structure on the vibration characteristics of the whole structure was investigated. It was found that the vibration performance was improved when the number of beams was increased and adjacent ALC floor panels were bonded to each other.

Keywords: numerical simulation; FEM; autoclaved lightweight aerated concrete (ALC); structural analysis

1. Introduction

In recent years, people have become more sensitive to noise against a background of increased time spent at home, so that the importance of sound environmental performance in buildings is increasing [1]. Floor impact noise is considered to be the most irritating noise for residents [2–4]. Floor impact sounds are divided into two types, namely light- and heavyweight floor impact sounds. The former noise can be easily dealt with after construction, while the latter requires structural measures to reduce it, but these measures are difficult and expensive to implement after construction is complete. Therefore, estimation of the floor vibration performance at the structural design stage is an effective means for producing an appropriate environmental design.

Regarding numerical simulation technology in the field of buildings, it is effective not only for floor vibration but also for many other aspects. For example, a numerical simulation study of a typical reconstruction house showed that seismic performance of masonry wall can be greatly improved by being wrapped in reinforced concrete or seismic band [5]. It has also been used to establish a precise and concise formula for quantifying the out-of-plane flexural capacity and initial stiffness of unstiffened eccentric steel rectangular hollow section (RHS) X-connections [6], and to help investigate the properties of diagrid structures [7,8]. In terms of floor impact noise, various studies have reported on prediction methods for floor impact sound insulation characteristics of reinforced-concrete buildings [9–24]. In these studies, an energy-based method, such as statistical energy analysis (SEA) [20–22], and a wave-based method, such as the finite-element method (FEM) or the finite-difference time-domain method [23,24] are used to simulate vibration propagation in the structure. SEA is quite efficient from the viewpoint of lower calculation costs. However, it is more straightforward to model and discretize the object of the simulation target by a wave-based discrete numerical approach. Among them, FEM is especially used for structural analysis. Some research on predicting the vibration characteristics of steel-framed structures has also been conducted [25–28]; however, almost all studies targeted the prediction of the vibration characteristics of a building structure, and their numerical results included very low-frequency components excited by, for example, seismic vibration. In contrast, floor impact sound includes relatively higher-frequency components up to at least 500 Hz, which requires quite detailed modeling of the steel-framed structure. In such a frequency range, the vibration characteristics are more complex because the wavelength of the propagated bending wave is smaller. The detailed characteristics of steel-framed structures have been experimentally investigated [29–33], and the results described the effect of the steel-framed walls and floors on the vibroacoustic transmission characteristics. In steel-framed structures, not only slab plates but also steel-frame structures, including beams and columns, have a large impact on the total structure-borne sound transmission characteristics of the building, compared to the simple situation of reinforced-concrete structures where the structure consists of relatively few materials. However, the influence of such complex mechanisms has not yet been sufficiently investigated. Furthermore, it has been suggested that a practical and efficient design method to evaluate the vibration serviceability of cold-formed steel floor systems is not yet available [33]. To address these problems, it is necessary to study the characteristic differences in sound insulation caused by differences in construction details, and not only experimental but also numerical investigations will play a role in determining these differences.

Examples of existing studies on numerical prediction methods for floor impact sound insulation performance of steel-framed buildings include the application of a finite element analysis to steel-framed buildings [34] and the application of a coupled displacement in-plane and out-of-plane to deck plate slabs [35,36]. Comprehensive analytical and experimental studies on equivalent rigidities of steel floor systems for vibration analysis based on an orthotropic plate model have been presented, and the fundamental frequencies of the structure have been validated as basic studies [37,38]. Further, Abramowicz et al. recently investigated a detailed method of treating the numerical coupling scheme between the slab and I-shaped steel beams [39]. In these cases, the vibration characteristics of steel-framed structures were simulated by FEM and the modal characteristics of the structure were discussed, but detailed validation of the frequency responses of vibration at higher frequency ranges, which can be applied to practical prediction, has not yet been sufficiently treated. Thus, further practical studies are needed to improve the accuracy of the simulations and expand the range of applications.

This study investigated the numerical prediction of the vibration characteristics of a steel-framed floor structure with autoclaved lightweight aerated concrete (ALC) plates using FEM. ALC is a lightweight cellular concrete building material mainly made of silica stone, cement, quicklime, and aluminum powder. The density and elasticity of ALC panels are much lower than those of reinforced-concrete panels. Therefore, despite their low cost, ALC floor structures may suffer from sound insulation weaknesses that require an adequate sound insulation design. However, by using the numerical procedure described above, it is possible to improve the floor-impact-sound insulation characteristics by considering the vibration mechanism of the complex structure consisting of the panels and frame structure. However, there have been not yet been any previous study of sound insulation improvement of steel-framed ALC floor structures, and it is novel to clarify the mechanism of how the floor-impact-sound characteristics are affected by the panel size and beam structure.

In this paper, the applicability of FEM to steel-framed ALC floor structures was confirmed by comparison with measurement results. In this study, experimental investigation was conducted to obtain measurement data for comparison to confirm the validity of the numerical results. Recently, a novel vibration measurement technique of non-contact measurement of vibration using a laser doppler vibrometer system [40,41] has been investigated. This method can eliminate the influence of the mass loading of the accelerometer, and has the possibility to be adopted for floor-impact-sound measurement. However, in this study, the measurement target was heavy enough not to be affected by the mass of the accelerometer, and a large amount of the former experimental results in the field of floor vibration have been obtained by using the hammering method. Therefore, the conventionally used impact hammer measurement method was adopted for validation. Then, the effect of sound insulation measures on a steel-framed ALC floor structure was discussed through numerical studies.

2. Measurements

2.1. Methods

Schematics of the ALC setup for a span of the target building showing measurement points and the beam plan is shown in Figure 1. A photograph of the measurement setup is shown in Figure 2a. The target building is a three-story steel-framed structure. The target for measurement is a span of the second floor. When the measurements were carried out, construction of the steel-frame structure and the separation walls had been completed, but interior elements had not yet been installed. Thus, only the vibration characteristics of the steel frame with ALC plates were measured. The ALC floor panels had a thickness of 100 mm. Note that each ALC panel had a different size, and appropriate pairs of panels with different sizes were chosen for each span structure. Each ALC floor panel was connected to the steel beam at two points using the mounts shown in Figure 2b. The steel frame was made of light-gauge steel.

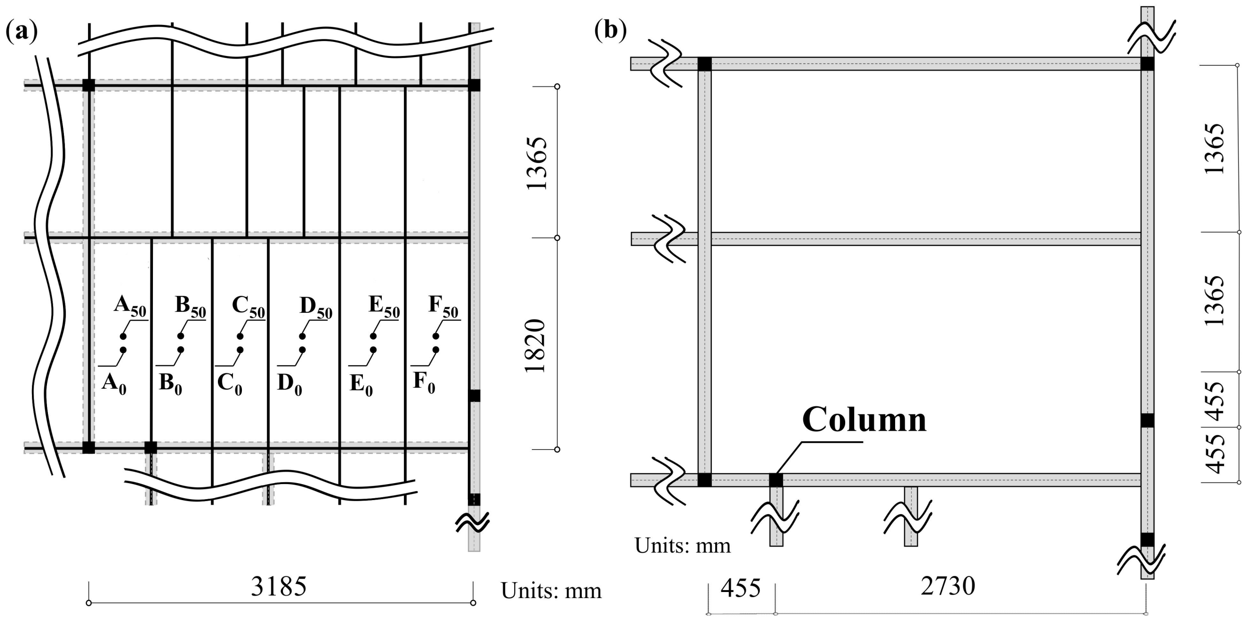

Figure 1. (**a**) Setup of ALC panels and arrangement of vibration receiving and source points; (**b**) beam plan of steel-frame structure.

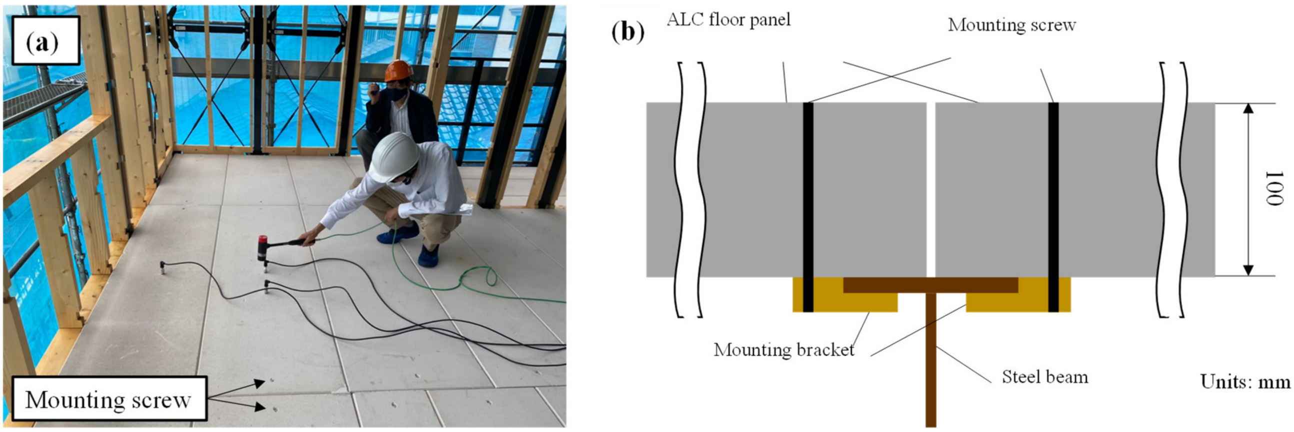

Figure 2. (**a**) Photograph showing hammering of ALC panels; (**b**) detailed cross-sectional schematic around mounts connecting ALC floor panels to steel beam.

Acceleration was measured at receiving points A_{50} to F_{50} when source points A_0 to F_0 were vibrated. Here, source points A_0 to F_0 were located at the center of each ALC floor panel, while the receiving points A_{50} to F_{50} were 50 mm from the center. The source points on the ALC plates were excited by an impact hammer. A PC-connected fast Fourier transform analyzer (OROS, OR34J-4) was used for real-time measurements of acceleration by hammering. A rising trigger was set for the measurement with 3 N as the threshold. The sampling frequency was 12,800 Hz and 1.28 s of measurement data was used to obtain the FFT analysis results. The frequency resolution of the acquired FFT analysis results is 0.78125 Hz. The voltage sensitivity of the impact hammer used for the measurements was 0.2492 mV/N, and the voltage sensitivity of the accelerometer was 10.7 mV/m/s^2.

2.2. Results

The measurement results at the six receiving points are shown in Figure 3. Because the steel-framed structure using light-gauge steel is relatively flexible compared with a more rigid structure, such as a reinforced-concrete structure, the lightweight structure may cause nonlinearity. Therefore, the excitation measurement was first performed four times while changing the input force at all measurement points to evaluate the influence of the nonlinearity of the particle damping characteristics. By comparing these results even if the input force changes, the accelerance in the frequency range of 10 Hz to 1 kHz obtained at the receiving points were mainly unchanged, confirming that these ALC structures exhibit sufficient linearity for the range of forces used. Although the sound insulation improvement of low frequency range under 100 Hz is important from the viewpoint of heavy floor impact sound characteristics, the frequency characteristics under 10 Hz are not basically perceived as sounds and are not treated in the field of acoustics for floor impact sound transmission. Note that the prediction of floor vibration under 10 Hz is of great importance from the viewpoint of body sensation of vibration. So, this paper focuses on the vibroacoustic characteristics in the acoustic frequency domain from 10 to 1000 Hz.

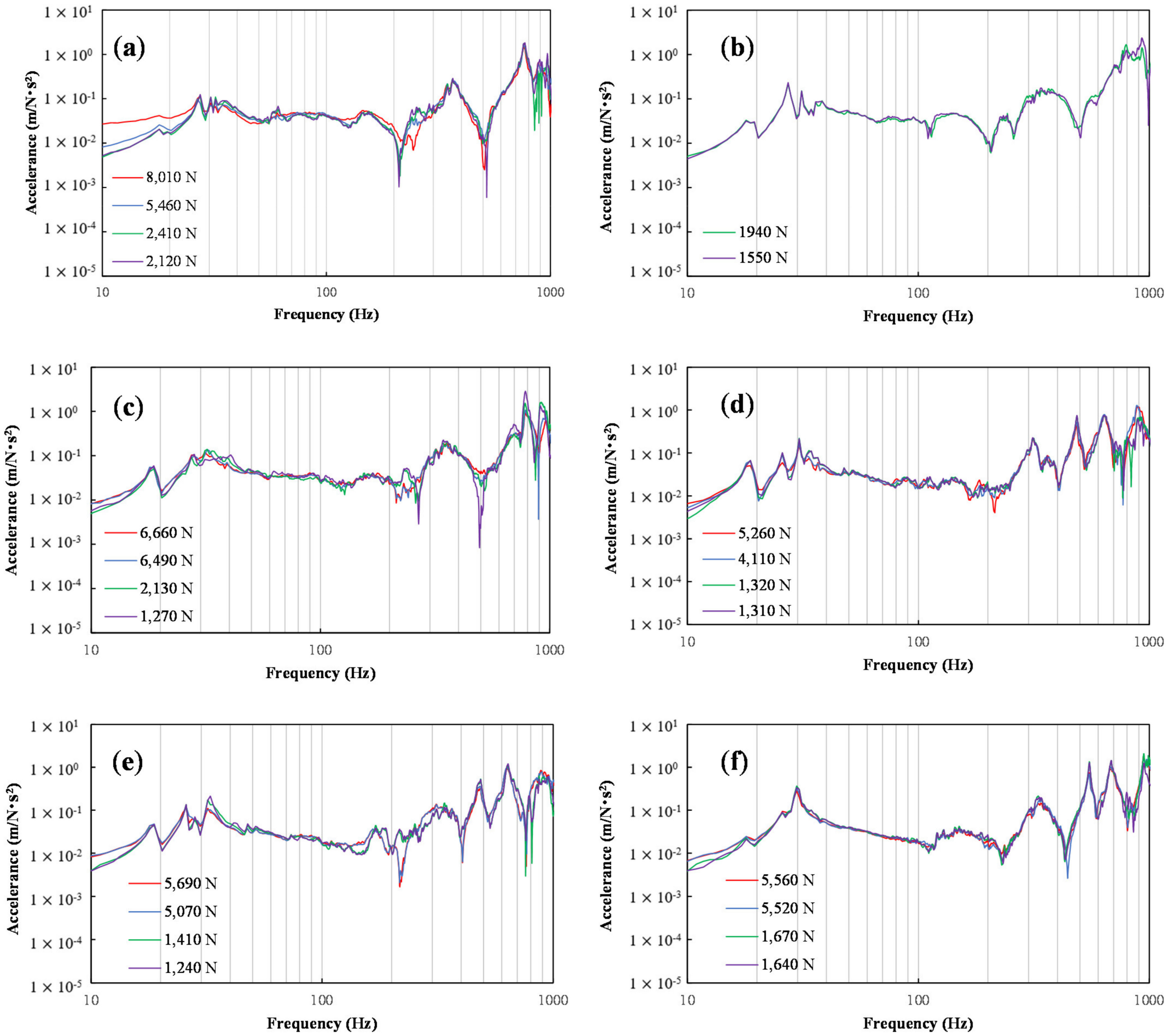

Figure 3. Measurement results for accelerance at six receiving points: (**a**) A_{50}, (**b**) B_{50}, (**c**) C_{50}, (**d**) D_{50}, (**e**) E_{50}, and (**f**) F_{50}.

3. Numerical Simulations

To verify the numerical results, the frame structure with ALC panels was numerically modeled using FEM, and the vibration characteristics were calculated and compared to the measurement results reported in the previous section.

3.1. Numerical Method

The numerical model was generated by simulating only one span of the measured building, as shown in Figure 4. Beam elements were used to model the columns and beams, and shell elements were used to model each of the ALC floor panels. Each ALC floor panel was connected to the beam by rigid elements at two points as shown in Figure 2b. As a constraint condition, a fixed edge condition was set at the lowest node of the column to model the column as standing on rigid ground. The other boundaries of the ALC panels were simulated as free boundaries. The numerical parameters used in the simulations are shown in Table 1. Because ALC can have a wide range of densities according to the production method [42], in this study, the parameters for ALC floor panels were determined based on the Japanese ALC panel structure design guideline and commentary [43], which is a technical standard in Japan to maintain and improve the quality of buildings using ALC panels.

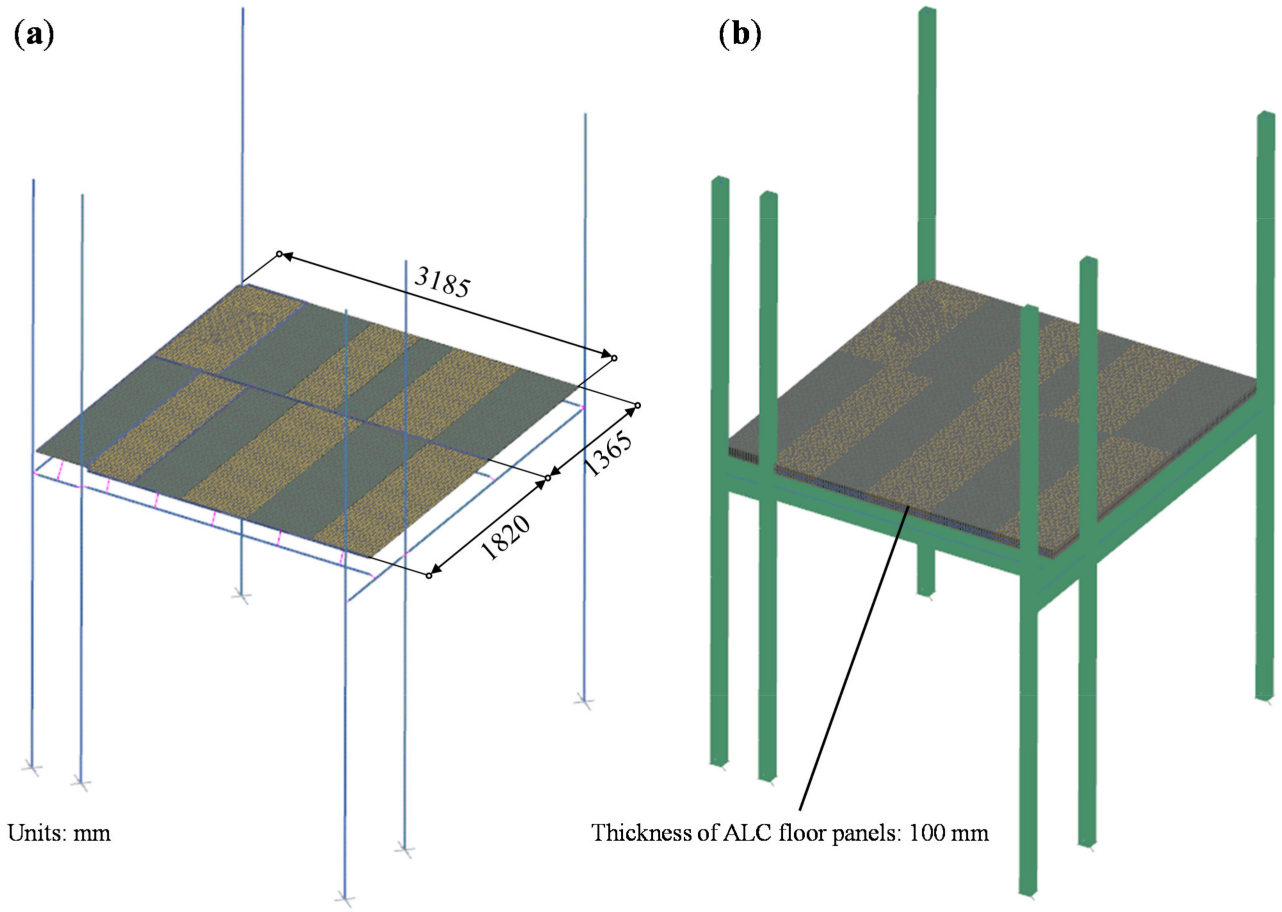

Figure 4. (**a**) Numerical model with beams and columns modeled using beam elements; (**b**) original view of structure illustrating thickness and cross-sectional shape of beams and columns.

Table 1. Numerical parameters adopted in FEM simulations.

Property	ALC Floor Panels	Columns and Steel Frames
Young's modulus	1.75×10^9 N/m^2	2.00×10^{11} N/m^2
Poisson's rato	0.2	0.3
Density	650 kg/m^3	7850 kg/m^3
Damping ratio	0.03	0.02

3.2. Comparison of Measurement and Simulation Results

Comparisons between the measurement and simulation results at the six receiving points are shown in Figure 5. The measurement points are as shown in Figure 1, and Figure 5 reports the accelerance at A_{50} to F_{50} when the center of each ALC floor panel (A_0 to F_0) was vibrated. Although there is a difference in the magnitude of the response at the peak frequency between the measurement and simulation results, and further improvement of the simulation accuracy would be desirable, all numerical results show a similar trend to the measurement results. Therefore, the validity of the modelling method is confirmed.

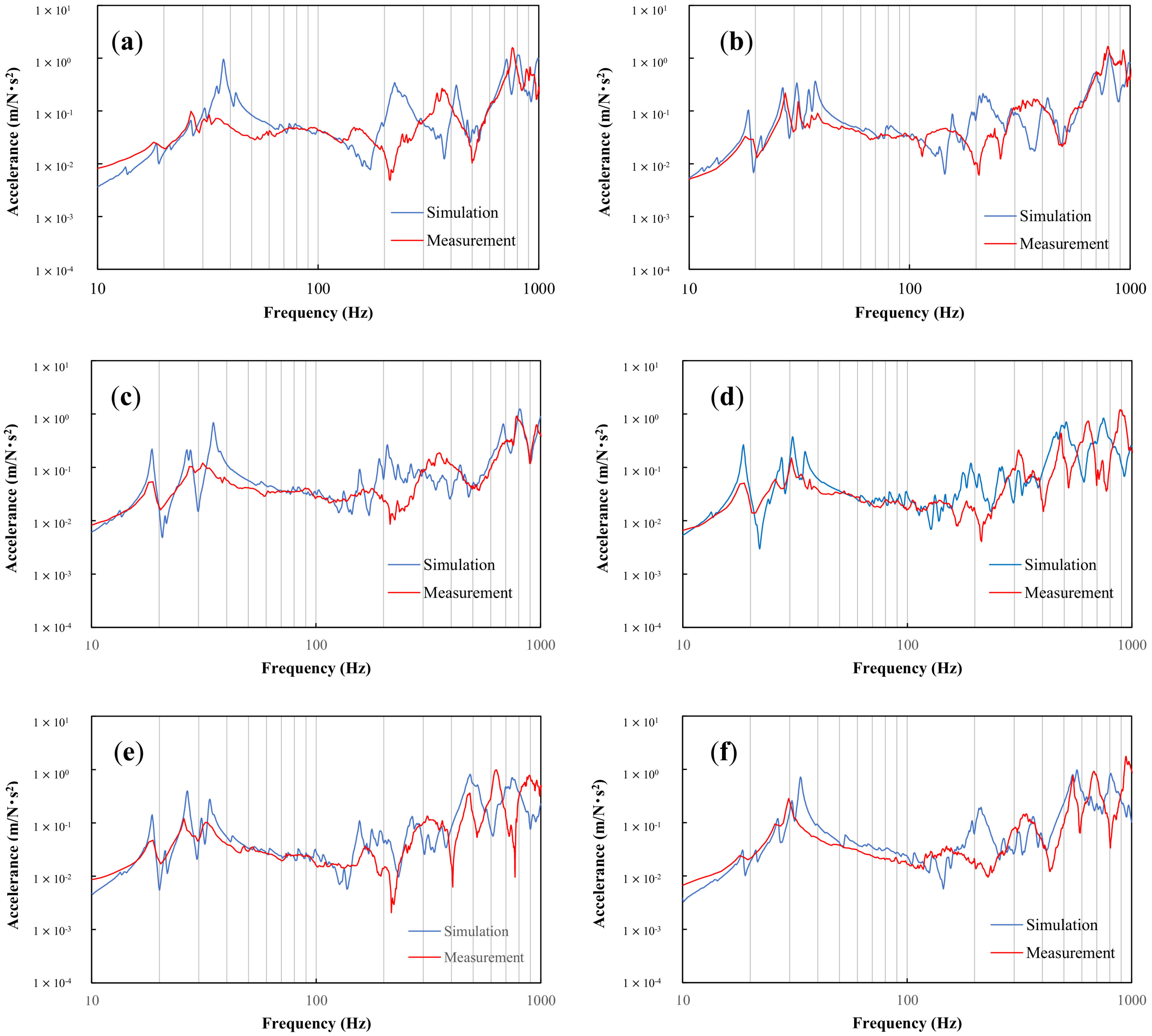

Figure 5. Comparisons of measurement and simulation results at six measurement points: (**a**) A_{50}, (**b**) B_{50}, (**c**) C_{50}, (**d**) D_{50}, (**e**) E_{50}, and (**f**) F_{50}.

4. Case Studies

This section describes how the vibration characteristics of steel-framed ALC floor panels were investigated using the validated numerical prediction method. In Sections 4.1 and 4.2, the effects of ALC floor panel size and beam structure on the vibration characteristics are discussed by comparing the results obtained from different numerical models. Then, in Sections 4.3 and 4.4, to investigate measures to increase the sound insulation characteristics, the effect of the number of beams used to form the frame structure and the effect of bonding adjacent panels and integrating the overall ALC panels are evaluated by comparing the results with previously measured results obtained by Sho et al. [44].

4.1. Effect of ALC Floor Panel Size

Two numerical models were used to investigate the effect of ALC floor panel size on the vibration characteristics. The thickness of all ALC floor panels was 100 mm. The numerical models are shown in Figure 6. The excitation and receiving points are indicated by red dots.

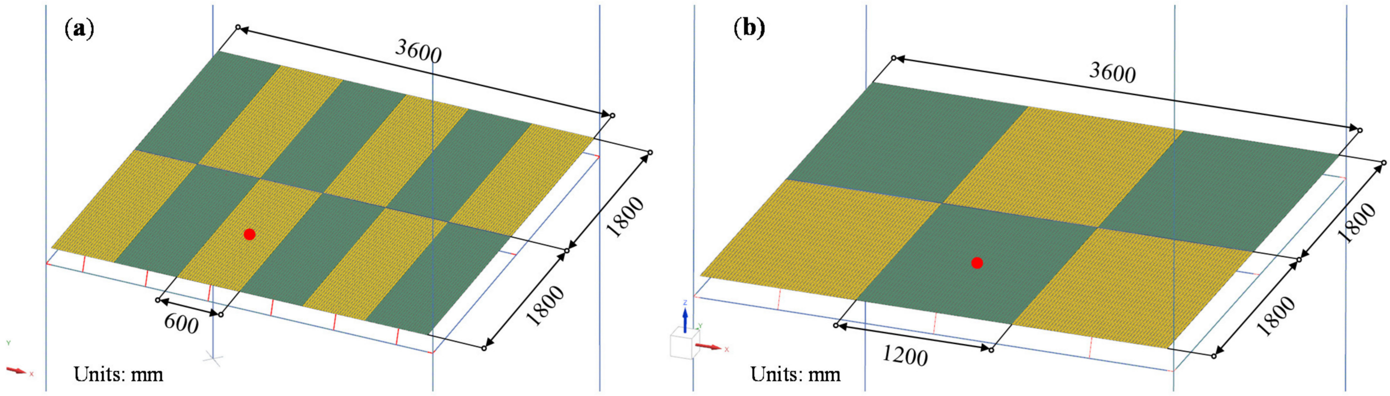

Figure 6. (**a**) Basic numerical model; (**b**) modified numerical model with different ALC floor panel sizes but same frame structure as in model (**a**).

The numerical results are shown in Figure 7, which shows that no significant difference was seen at frequencies lower than 30 Hz, despite the different sizes of the ALC floor panels. However, at frequencies higher than 30 Hz, the difference is large.

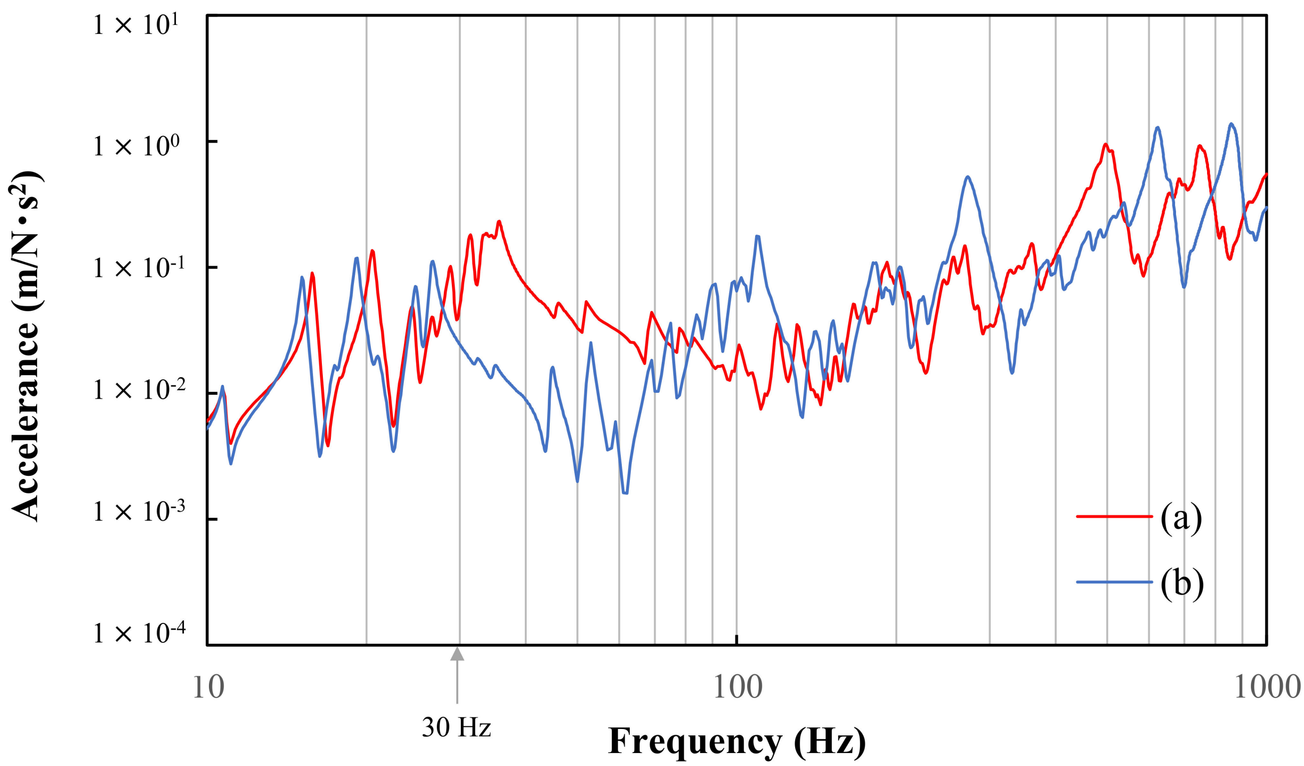

Figure 7. Effect of size of ALC floor panels on acceleration characteristics. Condition (**a**) is the numerical model with the basic-size ALC floor panels, while (**b**) is the numerical model with large ALC floor panels.

4.2. Effect of Beam Structure

Two numerical models were used to investigate the effect of the beam structure on the vibration characteristics. The size of each ALC floor panel was the same for both numerical models, with a thickness of 100 mm. The numerical models are shown in Figure 8. The excitation and receiving points are indicated by red points.

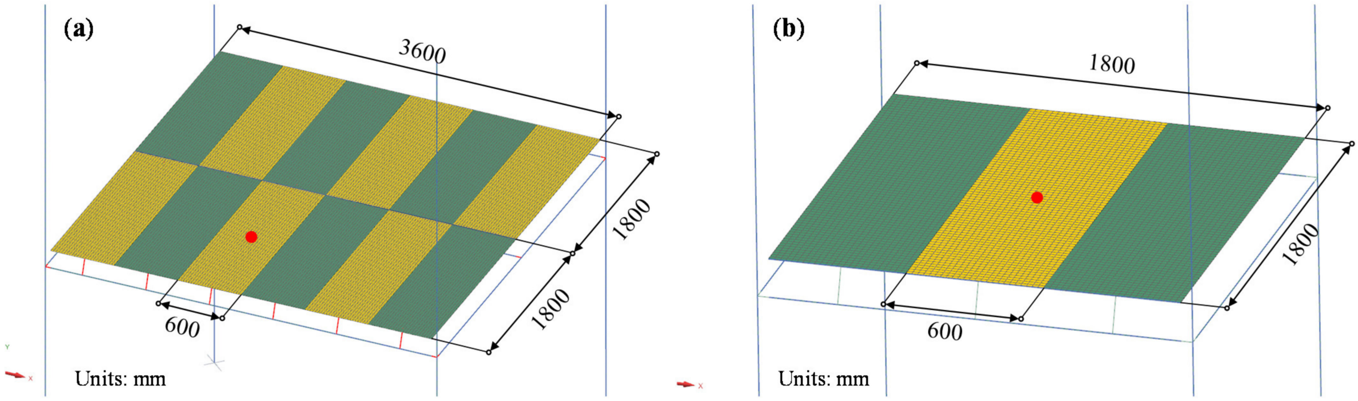

Figure 8. (**a**) Basic numerical model; (**b**) modified numerical model with different beam structure but the same ALC panel size.

The numerical results are shown in Figure 9, which shows that no significant difference is seen at frequencies higher than 30 Hz, despite the different beam structures. However, at frequencies lower than 30 Hz, the difference is large.

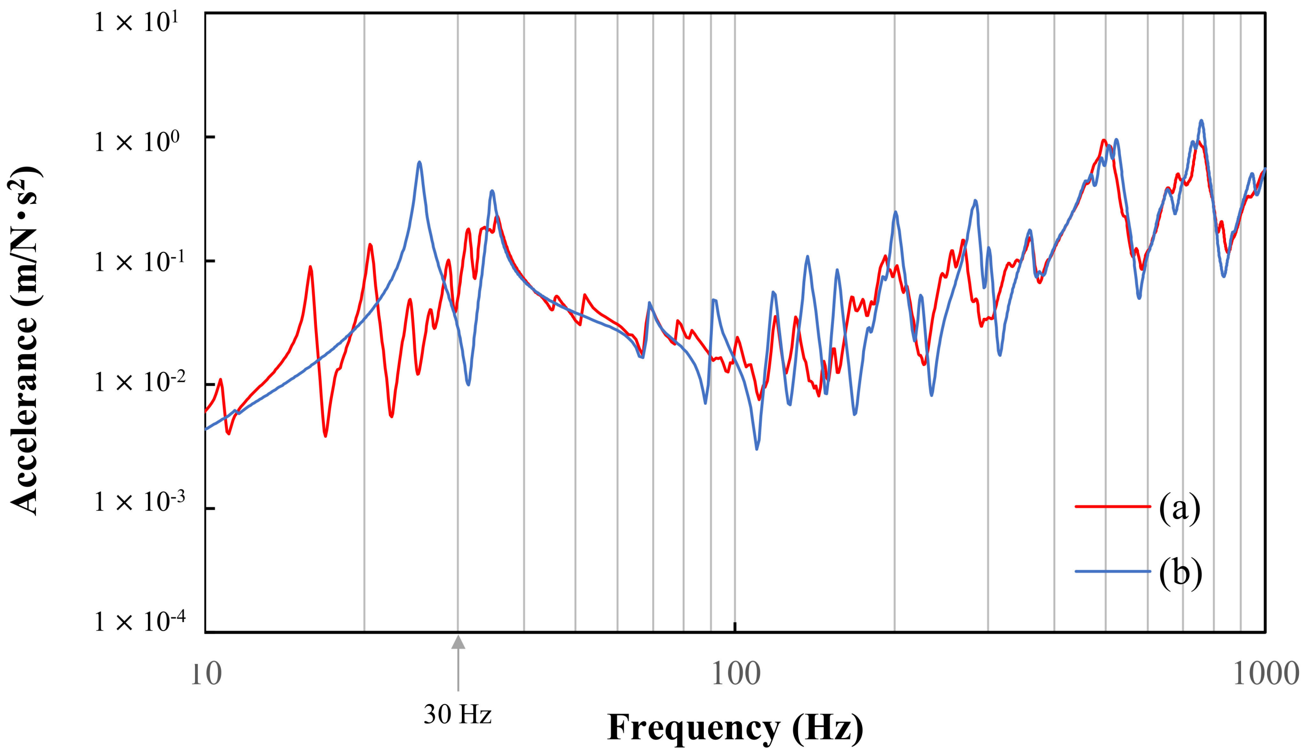

Figure 9. Effect of beam structure on accelerance characteristics. Condition (**a**) is the numerical model with a basic beam structure, while (**b**) is the numerical model with a small beam structure.

4.3. Effect of Number of Beams

Two numerical models with different numbers of beams were used, and the results were compared with those of previous measurements [44]. The numerical models are shown in Figure 10. The excitation and measurement points are indicated by red dots.

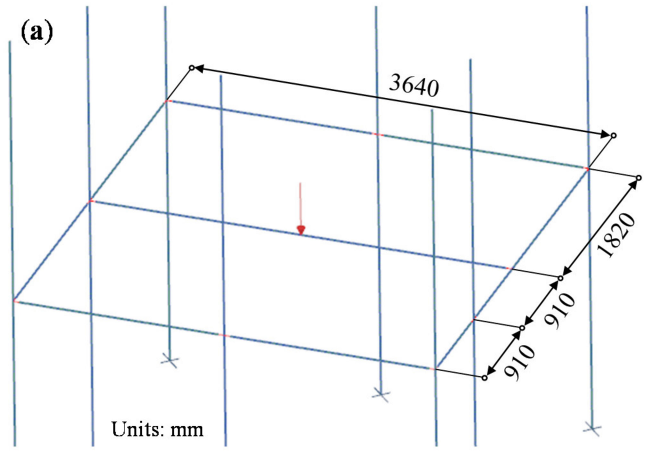

Figure 10. Schematics of (**a**) beam structure 1 and (**b**) beam structure 2.

The numerical results for mobility are shown in Figure 11. It can be seen that below about 300 Hz, a similar reduction in mobility is observed with increasing number of beams in both the simulation and experimental results.

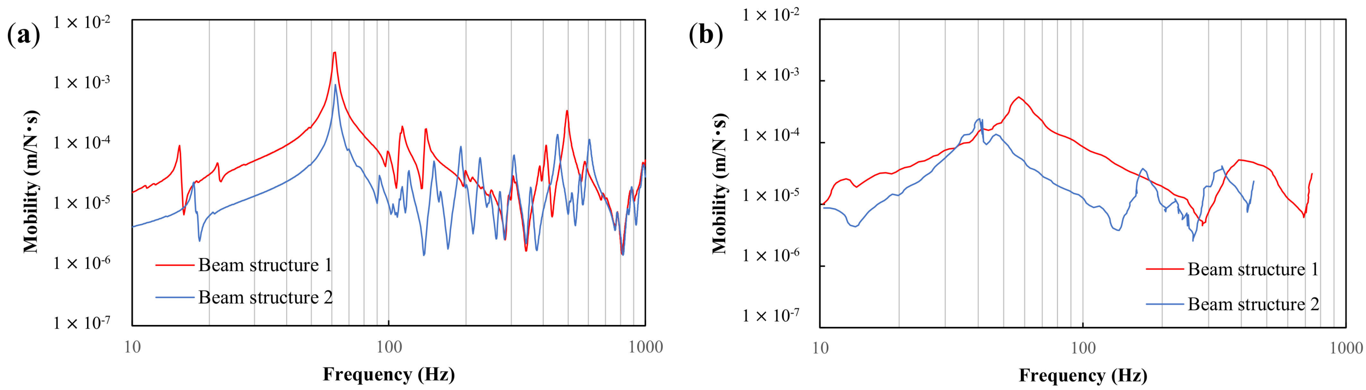

Figure 11. (**a**) FEM results obtained in present study; (**b**) measurement results from Sho et al. [44].

4.4. Effect of Bonding of Adjacent Panels

Numerical simulations were carried out for numerical models with bonding between adjacent ALC floor panels by rigid element or by spring element in addition to that with no bonding. Spring elements with spring constant of 50 N/mm were set at the points with an interval every 12.5 mm. The spring constant was set assuming that a rubber sealing with a thickness of 30 mm that has hardness of Hs60~Hs70 is sandwiched between the adjacent area of the ALC floor panel. Then, a numerical model with 12 sheets of ALC floor panels, as shown in Figure 7a, was set and the changes in vibration characteristics due to bonding were compared with the results of previous measurements [44].

The numerical results are shown in Figure 12. Further, the results obtained in 1/1 octave band are also shown in Figure 13, which also shows the results of mobility for the conditions with spring constants of 10 and 100 N/mm as well as 50 N/mm for reference. These plots show that below 100 Hz, both the simulation and measurement results indicate a similar reduction in mobility due to bonding. It was also confirmed that below 100 Hz, the mobility was more damped as the bonding by the spring elements was stiffer. While the tendency is different in the high frequency range, heavy floor impact sounds are predominantly in the low frequency range, and it is important to reduce vibration levels in the low frequency range. So, the above findings, where the floor impact sound characteristics can be controlled by bonding the adjacent panels by some materials like rubber, can be applied to practical sound insulation planning of buildings.

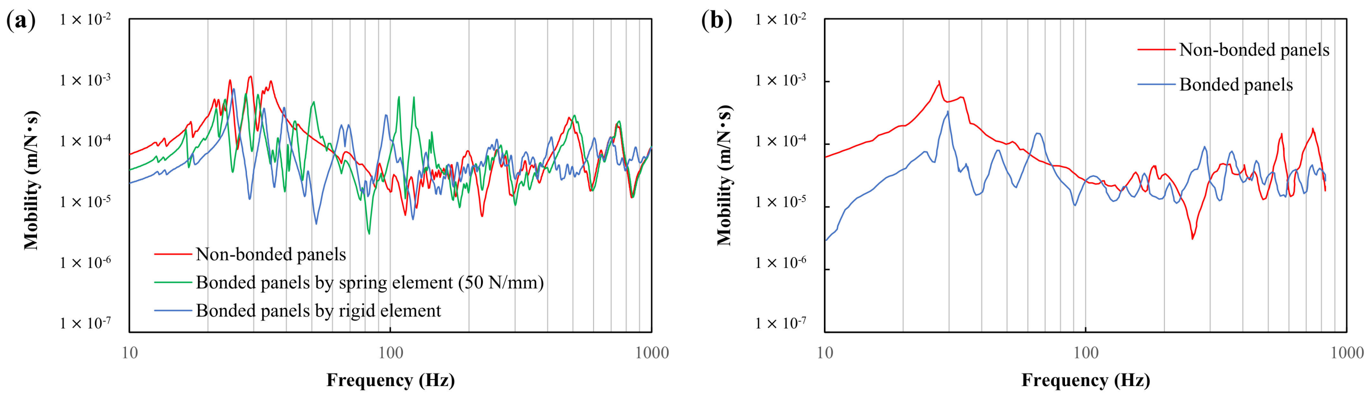

Figure 12. (**a**) Numerical result by the FEM in the present study; (**b**) measurement results from Sho et al. [44].

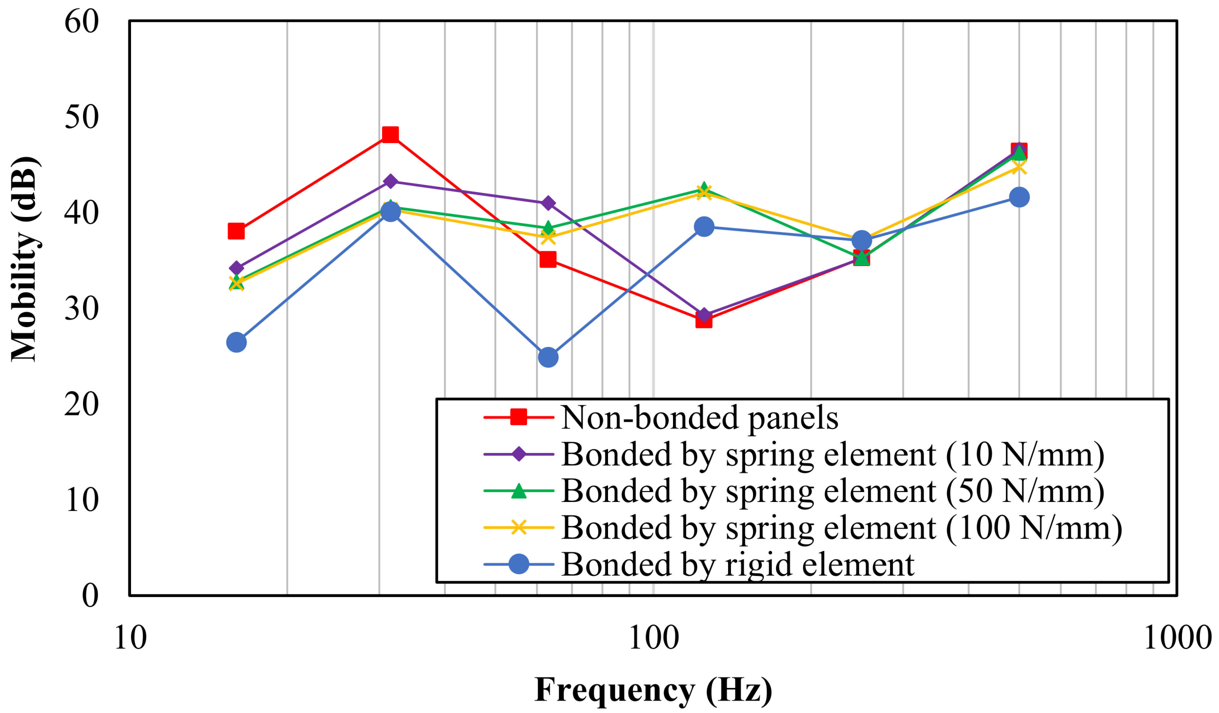

Figure 13. Results of octave band analysis of numerical result by the FEM in the present study.

The results reported here show that increasing the number of beams and bonding adjacent panels may be effective measures against propagation of heavy floor impact sounds in steel-framed structures with ALC panels.

5. Limitations

In this study, the validity of an FEM-based prediction method for ALC steel-framed structures was verified through a comparison with the numerical results for models of these structures. However, only the vibration characteristics for a single floor were considered; thus, the accuracy of the proposed method for multiple floors should be investigated in a future study. However, the case considered in the present study has a basic frame geometry, and the knowledge obtained should be applicable to vibration prediction for other geometries. As described in Section 4, the influences of the ALC plate dimensions, the division of the steel-frame geometry, and the presence or absence of bonding between

ALC panels on the vibration properties were investigated through numerical studies, and these findings are also considered to be fully applicable to other cases.

6. Conclusions

In the present study, the applicability of FEM to steel-framed ALC floor structures was examined by comparing simulation results with actual measurement results. Further, the mechanism for how the floor-impact-sound characteristics of the ALC floor structure decrease when affected by the panel size and beam structure was clarified using the validated numerical scheme. Based on the validation, the floor vibration can be predicted with high accuracy by creating a discrete numerical model using beam elements for columns and beams, and shell elements for ALC floor panels. Next, numerical case studies were carried out to determine the effects of the ALC floor panel size and the beam structure on the vibration characteristics. The results confirmed that doubling the panel width for the panel sizes conducted in this study had little effect on the vibration characteristics at frequencies lower than 30 Hz, while changes in the beam structure had a significant effect on the vibration characteristics at frequencies below 30 Hz. The effects of the number of beams and of bonding between adjacent ALC panels were also investigated. The simulation results indicated that increasing the number of beams and elastically bonding panels together improved the vibration characteristics at low frequencies.

Author Contributions: Conceptualization, H.M.; methodology, H.M.; investigation, H.M.; resources, Y.I. and T.S.; writing—original draft preparation, H.M.; writing—review and editing, H.M. and T.A.; visualization, H.M.; supervision, T.A. and F.S.; project administration, T.A. All authors have read and agreed to the published version of the manuscript.

Funding: This research received no external fundings.

Institutional Review Board Statement: Not applicable.

Informed Consent Statement: Informed consent was obtained from all subjects involved in the study.

Data Availability Statement: Not applicable.

Conflicts of Interest: The authors declare no conflict of interest.

References

1. Ryuta, T.; Kyoko, A. Questionnaire survey on sound environment of apartment houses during stay home by COVID-19. *AIJ J. Technol. Des.* **2021**, *27*, 1303–1308. (In Japanese)
2. Langdon, F.J.; Buller, I.B.; Scholes, W.E. Noise from neighbours and the sound insulation of party walls in house. *J. Sound Vib.* **1981**, *79*, 205–228. [CrossRef]
3. Langdon, F.J.; Buller, I.B.; Scholes, W.W. Noise from neighbours and the sound insulation of party floors and walls in flats. *J. Sound Vib.* **1983**, *88*, 243–270. [CrossRef]
4. Sho, K.; Katsuo, I.; Michiko, S.; Kazuhiro, F. Analysis of occupancy evaluation and behaviour as to multi-family dwelling sound environment. *AIJ J. Archit. Plann. Environ. Eng.* **1994**, *466*, 1–8. (In Japanese)
5. Liu, C.; Fang, D.; Zhao, L. Reflection on earthquake damage of buildings in 2015 Nepal earthquake and seismic measures for post-earthquake reconstruction. *Structures* **2021**, *30*, 647–658. [CrossRef]
6. Zhao, B.; Ke, K.; Liu, C.; Hong, L. Computational Model for the Flexural Capacity and Stiffness of Eccentric RHS X-Connections under Brace Out-of-Plane Bending Moment. *J. Struct. Eng.* **2020**, *146*, 04019227-1–04019227-15. [CrossRef]
7. Liu, C.; Fang, D.; Zhao, L.; Zhou, J. Seismic fragility estimates of steel diagrid structure with performance-based tests for high-rise buildings. *J. Build. Eng.* **2022**, *52*, 104459. [CrossRef]
8. Liu, C.; Fang, D. Robustness analysis of vertical resistance to progressive collapse of diagrid structures in tall buildings. *Struct. Des. Tall Spec. Build.* **2020**, *29*, e1775. [CrossRef]
9. Sho, K.; Katsuo, I. Practical calculation of floor impact sound by impedance method. *Appl. Acoust.* **1989**, *26*, 263–292.
10. Norihisa, H.; Mitsuhiro, K. Sound insulation of a rectangular thin membrane with additional weights. *Appl. Acoust.* **1991**, *33*, 21–43.
11. Carl, H. Prediction of maximum time-weighted sound and vibration levels using transient statistical energy analysis. Part 1: Theory and numerical implementation. *Acta Acust. United Acust.* **2014**, *100*, 46–54.
12. Carl, H.; Matthew, R. Prediction of maximum time-weighted sound and vibration levels using transient statistical energy analysis. Part 2: Experimental validation. *Acta Acust. United Acust.* **2014**, *100*, 57–66.

13. Susume, H.; Carl, H.; Pyoung, J.L. Impact sound insulation: Transient power input from the rubber ball on locally reacting mass-spring systems. In Proceedings of the Inter-Noise 2016, Hamburg, Germany, 21 August 2016.
14. Susume, H.; Carl, H.; Pyoung, J.L. Comparison and assessment of Japanese, Korean and international measurement procedures for impact sound insulation with heavy impact sources. In Proceedings of the ICSV25, Hiroshima, Japan, 8–12 July 2018.
15. Susume, H.; Carl, H. Prediction of heavy impact sounds using transient statistical energy analysis and finite element methods. In Proceedings of the ICSV25, Hiroshima, Japan, 8–12 July 2018.
16. Yukiko, H.; Hikari, T.; Atsushi, T. Investigation method of heavy weight floor impact sound of large span slab focused on modeling procedure of the finite-element method. *Rep. Taisei Tech.* **2005**, *38*, 45-1–45-4. (In Japanese)
17. Norihisa, H. Dynamical analysis in audio-frequency range of the beam-slabs by fem Study on floor slab vibrations and sound radiation Part 1. *AIJ J. Archit. Plann. Environ. Eng.* **1987**, *372*, 1–9. (In Japanese)
18. Atsushi, N. Study on vibration and application of simulation technique for the floor impact sound based on both FEM floor vibration analysis and BEM sound field analysis. *AIJ J. Archit. Plann. Environ. Eng.* **1990**, *521*, 33–40. (In Japanese)
19. Takashi, K.; Masanori, T.; Kei, A. Investigations on the prediction method of floor impact sound for large-span slabs focused on aspect ratio of slab plan. *AIJ J. Archit. Plann. Environ. Eng.* **2000**, *537*, 13–19. (In Japanese)
20. Craik, R.J.M.; Steel, J.A.; Evans, D.I. Statistical energy analysis of structure-borne sound transmission at low frequencies. *J. Sound Vib.* **1991**, *144*, 95–107. [CrossRef]
21. Churchill, C.; Hopkins, C. Prediction of airborne sound transmission across a timber–concrete composite floor using statistical energy analysis. *Appl. Acoust.* **2016**, *110*, 145–159. [CrossRef]
22. McCollum, M.D.; Cuschieri, J.M. Bending and in-plane wave transmission in thick connected plates using statistical energy analysis. *J. Acoust. Soc. Am.* **1990**, *88*, 1480–1485. [CrossRef]
23. Toyoda, M.; Takahashi, D. Prediction for architectural structure-borne sound by the finite-difference time domain method. *Acoust. Sci. Technol.* **2009**, *30*, 265–276. [CrossRef]
24. Asakura, T.; Ishizuka, T.; Miyajima, T.; Toyoda, M. Numerical and experimental investigation on structure-borne sound transmission in multilayered concrete structures. *J. Sound Vib.* **2018**, *413*, 1–25. [CrossRef]
25. Miyamura, T.; Ohsaki, M.; Kohiyama, M. Large-scale FE analysis of steel building frames using e-simulator (Selected papers of the Joint International Conference of Supercomputing in Nuclear Applications and Monte Carlo: SNA + MC 2010). *Prog. Nuc. Sci. Tech.* **2011**, *2*, 651–656. [CrossRef]
26. Miyamura, T.; Yamashita, T.; Akiba, H.; Ohsaki, M. Dynamic FE simulation of four-story steel frame modeled by solid elements and its validation using results of full-scale shake-table test. *Earthq. Eng. Struct. Dyn.* **2015**, *44*, 1449–1469. [CrossRef]
27. Tagawa, H.; Miyamura, T.; Yamashita, T.; Kohiyama, M.; Ohsaki, M. Detailed finite element analysis of full-scale four-story steel frame structure. *Int. J. High-Rise Build.* **2015**, *4*, 65–73.
28. Park, J.-W.; Ha, T.-H.; Kim, H. Finite element modeling and experimental verification of lightweight steel floor vibration. *J. Vibroeng.* **2016**, *18*, 1435–1443. [CrossRef]
29. Xu, L.; Tangorra, F.M. Experimental investigation of lightweight residential floors supported by cold-formed steel C-shape joists. *J. Constr. Steel Res.* **2007**, *63*, 422–435. [CrossRef]
30. Parnell, R.; Davis, B.; Xu, L. Vibration performance of lightweight cold-formed steel floors. *ASCE J. Struct. Eng.* **2010**, *136*, 645–653. [CrossRef]
31. Hoeller, C.; Zeitler, B.; Sabourin, I. Direct airborne and impact sound insulation of steel-framed floors for mid-rise constructions. In Proceedings of the Inter-Noise 2015, San Francisco, CA, USA, 9–12 August 2016.
32. Hoeller, C.; Zeitler, B.; Sabourin, I. *Airborne and Impact Sound Insulation Data for Cold-Formed Steel-Framed Walls and Floors*; Report A1-005007.1; National Research Council Canada: Ottawa, ON, Canada, 2018.
33. Zhang, S.; Xu, L. Vibration serviceability evaluation of lightweight cold-formed steel floor systems. *Structures* **2022**, *38*, 1368–1379. [CrossRef]
34. Hikari, T.; Kiyoshi, M. Floor impact sounds by heavy impact source in steel structure buildings—Vibrational properties of floor slabs and prediction using FEM. *Noise Cont.* **2012**, *36*, 425–434. (In Japanese)
35. Yu, A.; Norihisa, H. Study on natural vibration analysis of deck plate slabs and their conversion to flat plate -Numerical analysis on vibration and floor impact sound of deck plate slabs in steel structure buildings Part 1. *AIJ J. Technol. Des.* **2015**, *21*, 171–176. (In Japanese)
36. Yu, A.; Norihisa, H. Study on prediction of vibration response of deck plate slabs—Numerical analysis on vibration and floor impact sound of deck plate slabs in steel structure buildings Part 2. *AIJ J. Technol. Des.* **2016**, *22*, 153–158. (In Japanese)
37. Zhang, S.; Xu, L. Determination of equivalent rigidities of cold-formed steel floor systems for vibration analysis, Part I: Theory. *Thin-Walled Struct.* **2018**, *132*, 25–35. [CrossRef]
38. Xu, L.; Zhang, S.; Yu, C. Determination of equivalent rigidities of cold-formed steel floor systems for vibration analysis, Part II: Evaluation of the fundamental frequency. *Thin-Walled Struct.* **2018**, *132*, 1–15. [CrossRef]
39. Abramowicz, M.; Berczyński, S.; Wróblewski, T. Modelling and parameter identification of steel–concrete composite beams in 3D rigid finite element method. *Archiv. Civ. Mech. Eng.* **2020**, *20*, 103. [CrossRef]
40. Scislo, L.; Guinchard, M. Non-invasive measurements of ultra-lightweight composite materials using Laser Doppler Vibrometry system. In Proceedings of the 26th International Congress on Sound and Vibration, Montréal, QC, Canada, 7–11 July 2019.

41. Scislo, L. Quality assurance and control of steel blade production using full non-contact frequency response analysis and 3D laser doppler scanning vibrometry System. In Proceedings of the 11th IEEE International Conference on Intelligent Data Acquisition and Advanced Computing Systems: Technology and Applications, Cracow, Poland, 22–25 September 2021.
42. Narayanan, N.; Ramamurthy, K. Structure and properties of aerated concrete: A review. *Cem. Concr. Compos.* **2000**, *22*, 321–329. [CrossRef]
43. ALC Association. ALC Panel Structural Design Guideline and Commentary. 2013. (Translated from Japanese). Available online: http://www.alc-a.or.jp/pdf/alc_planguide.pdf (accessed on 20 September 2022).
44. Sho, K.; Katsuo, I.; Mitsuo, O. Methods for improving the performance of floor impact sound insulation for heavy impact source in steel frame ALC-type dwellings. *AIJ J. Archit. Plann. Environ. Eng.* **1997**, *496*, 15–21. (In Japanese)